High-voltage pulse crushing and physical separation of polycrystalline silicon photovoltaic panels

High-voltage pulse crushing and physical separation of polycrystalline silicon photovoltaic panels

Yuta Akimoto[1], Atsushi Iizuka[2,*] and Etsuro Shibata[2]

[1] *Graduate School of Environmental Studies, Tohoku University, 468-1, Aoba, Aramaki, Aoba-ku, Sendai, Miyagi, 980-0845, Japan*

[2]*Research Center for Sustainable Science and Engineering, Institute of Multidisciplinary Research for Advanced Materials, Tohoku University, 2-1-1, Katahira, Aoba-ku, Sendai, Miyagi, 980-8577, Japan*

*Correspondence concerning this article should be addressed to E. Shibata (Tel: +81 22 217 5214; Fax: +81 22 217 5214; E-mail: atsushi.iizuka.e4@tohoku.ac.jp)

Abstract

High-voltage pulse crushing technology combined with sieving and dense medium separation was applied to a photovoltaic panel for selective separation and recovery of materials. The panel was first separated into glass and back sheet layers by high-voltage pulse crushing through microexplosions or shock waves transmitted in the Al electrode and Si substrate (primary crushing step). Then the glass and bus-bar electrode could be separated from the encapsulant by high-voltage pulse crushing of the glass layer. The bus-bar electrode of the back sheet layer could also be separated by further high-voltage pulse crushing. After sieving the products obtained from the secondary crushing step of the glass layer, glass was mainly distributed in the size fraction range of 45–850 μm with a small amount of Si powder. However, purification of the glass (removal of Si powder) could be achieved by dense medium separation at a specific gravity of 2.4. Base metals, such as Cu, Sn, and Pb could be recovered in the large size fraction (1.0–8.0 mm). Ag used in the finger and bus-bar electrodes was highly condensed in the sieved product fraction with sizes of less than 20 μm, 2.0–4.0, and 4.0–8.0 mm, and its content exceeded 3000 mg/kg. However, the amount of Ag in these fractions represented only 33.2% of the total amount of Ag in the panel. Thus, to increase the Ag recovery ratio, other separation methods will be needed. We confirmed that dense medium separation at a specific gravity of 3.0 could achieve Ag condensation from the Si and glass, and that this represents a promising option for enhanced Ag recovery from crushed products.

Keywords: high-voltage pulse crushing, photovoltaic panel, selective crushing, recycling

Introduction

Photovoltaic power generation does not emit CO_2 gas while in use and represents an effective and secure energy source. Owing to the merits, installations of photovoltaic power generation systems have increased continuously to date (IEA-PVPS, 2017). The estimated lifetime of photovoltaic panels is 20–30 years (Goe and Gaustad, 2014); thus, the number of disposed panels is forecast to increase in the future (Weckend et al., 2016). Therefore, consideration of the disposal of photovoltaic panels is necessary. A silicon photovoltaic panel is composed of frames, a junction box, glass, encapsulant, a back sheet, and a photovoltaic cell, which consists of a Si substrate and Cu, Ag, and Al electrodes. Because photovoltaic panels contain valuable resources, recycling of the panels is required.

Recycling technologies for photovoltaic panel have been developing in recent years. There are three main approaches to recycling: mechanical (Bergera et al., 2010; Granata et al., 2014), thermal (Klugmann-Radziemska et al., 2010; Radziemska et al., 2010), and chemical (Doi et al., 2001; Klugmann-Radziemska and Ostrowski, 2010; Klugmann-Radziemska et al., 2010; Radziemska et al., 2010; Kim and Lee, 2012; Kang et al., 2012) methods. These methods have the following advantages and disadvantages. Mechanical methods are easy and low cost; however, the liberation of materials is poor compared with other methods. Thermal methods can remove the encapsulant, recover glass and the photovoltaic cell. However, the treatment cost of this method is high owing to the energy required for heating, and gas emitted while heating the encapsulant. Chemical methods can be used to separate glass and the photovoltaic cell with reduced contamination, such as that from the encapsulant; however, these treatments are high cost and require a relatively long

time. Therefore, the development of recycling technology to separate these materials with high efficiency and low cost is required, owing to the problems with the aforementioned methods of recycling photovoltaic panels. Thus, we have focused on a high-voltage pulse crushing technology, which has previously been applied to liquid crystal displays (Dodbiba et al., 2012), printed circuit boards (Duan et al., 2015; Zhao et al., 2015), and mineral ores (Wang et al., 2011; Wang et al., 2012). These studies have reported on the high performance of selective crushing technologies.

In this study, we apply high-voltage pulse crushing technology to photovoltaic panel crushing, combined with sieving and dense medium separation. The objective of this study was to establish a method for selective separation and recovery of materials in photovoltaic panels.

Materials

The subject of this study was recycling of a polycrystalline silicon photovoltaic panel. An end-of-life photovoltaic panel (1650 mm × 988 mm × 45 mm, 18.54 kg, 250 W) from a recycler was used for the experiments (Figure 1). First, the external frames and junction box were removed from the panel. We then manually cut the panel into squares with dimensions of 50 mm × 50 mm × 4.2 mm (approximately 20 g). Cut samples were used in the high-voltage pulse crushing experiments. A larger (wider) panel size is desirable to simplify the shredding treatment before electrical pulse crushing. We decided on this panel size (i.e., 50 mm × 50 mm × 4.2 mm) based on the maximum size that could fit at the bottom of crushing vessel.

Figure 1(a) and (b) show that an Al electrode was located under the Si substrate, and these layers were encapsulated in ethylene vinyl acetate (EVA). The encapsulant was sandwiched between glass and a back sheet, which had three layers. Figure 1(a) shows that Cu electrodes (bus-bar electrodes) were present on a Si substrate and an Al electrode. Solders (Sn and Pb) were found around the Cu electrodes. Ag electrodes (finger electrodes) were observed on the Si substrate, as shown in Fig. 1(b). Table 1 summarizes the material contents of each of the cut photovoltaic panel samples. The composition was estimated from elemental analysis of the cut panel samples with the use of inductively coupled plasma atomic emission spectrometry (ICP-AES; Spectro Arcos, Ametek Co. Ltd., Japan) after acid dissolution. Glass was the main component of the panel and its content was measured to be 78.4 wt%. The Si content was 4.0 wt%, and the Cu, Sn, and Pb contents of both the bus-bar electrodes were similar. More than 60% of the Ag content was contained in the other fraction, and this portion was related to Ag used in finger electrodes. The upper bus-bar electrode (upper surface side) contained three times as much Ag as that contain in the bottom side. It should be noted that this table does not include the contents of the back sheet layers and encapsulant.

Experimental

High-voltage pulse crushing experiments

High-voltage pulse crushing experiments were performed with a SELFRAG Lab S2.0 instrument (SELFRAG AG, Switzerland). After a piece of the cut panel was put on the bottom electrode in the vessel, the crushing experiments were conducted under the conditions listed in Table 2. The discharge voltage and gap between the electrodes

determines the potential gradient across the panel sample and surrounding water for electrical breakdown. In our high-voltage pulse crushing experiments, the gap between the electrodes was set to be 20 mm; however, for a discharge voltage of 90 kV the gap was set to be 10 mm because electrical breakdown did not occur when the distance was set at 20 mm. The discharge frequency was set to be 5 Hz for all conditions.

The panels were separated into two layers in the primary crushing step, as described below. To elucidate the separation mechanism of the panel into two layers, we observed fracture surfaces after the primary crushing step, under the optimal conditions, by scanning electron microscope (SEM; VE-9800, Keyence, Japan) and energy-dispersive X-ray spectroscopy (EDX; EDAX Genesis, Ametek Co. Ltd., Japan). Each layer was then crushed under the conditions summarized in Table 3. The obtained products were observed visually at appropriate times.

The product obtained by crushing under the optimal conditions was sieved through 11 different sieves (20, 45, 90, 150, 300, 500, and 850 μm, and 1.0, 2.0, 4.0, and 8.0 mm). The concentrations of Ag, Al, Ca, Cu, Mg, Na, Pb, Si, and Sn in each particle size range were determined by ICP-AES after dissolution by acid (HNO_3, HF, and H_3BO_3) with the use of an Ecopre system® (ACTAC, Japan). Undissolved encapsulant was removed by filtering with a PTFE filter (pore size: 0.2 μm) before the ICP-AES analysis. Partial sampling of the sieved products by the method of quartering was conducted for ICP-AES analysis of the size fractions of 20–45, 45–90, 90–150, 150–300, 300–500 and 500–800 μm. Whole samples were dissolved and analyzed for the size fractions of –20 μm and 2.0–4.0 mm. For the size fractions of 1.0–2.0, and 4.0–8.0 mm, the bus-bar electrode and encapsulant were

manually separated, and whole amount of the bus-bar electrode was dissolved and analyzed separately. For the size fraction of 1.0–2.0 mm, the remaining glass fraction was further ground in a mortar, and 100 mg of the resulting fine powder was taken and dissolved for ICP-AES analysis. For the size fraction of >8.0 mm, encapsulant to which a small amount of Si powder was adhered, was separated manually, and approximately 100 mg of this encapsulant was taken and analyzed. The weights of the materials were estimated from the results of the elemental analysis.

Dense medium separation experiments

Solutions for dense medium separation (2.4 and 3.0 g/cm^3) were prepared with the use of sodium polytungstate (85.6%, Wako Pure Chemical Industries) and distilled water. After dense medium separation, the light and heavy products were recovered from the solution. The recovered products were dissolved in acid (HNO_3, HF, and H_3BO_3), and the concentrations of Ag, Al, Ca, Cu, Mg, Na, Pb, Si, and Sn in the products were determined by ICP-AES. The weights of materials were estimated from the results of elemental analysis.

Results and Discussion

High-voltage pulse crushing

Primary crushing step

Figure 2 shows the products obtained from the primary crushing step. The panels were separated into a glass layer (left) and back sheet layer (right) under two sets of conditions

(110 kV for 20 pulses and 180 kV for 10 pulses) in an Al electrode and Si substrate. In particular, samples crushed under the former conditions retained its form unlike those crushed under the latter. From these results, we decided that 110 kV and 20 pulses were the optimal conditions for separating the panel into two layers because mutual separation before destruction of each material would be ideal for recycling of each material when considering the handling properties of crushed products and prevention of contamination. We considered that there are two main disintegration mechanisms in high-voltage pulse crushing, namely, electrical disintegration (ED) and electrohydraulic disintegration (EHD). In the ED mechanism, breakdown occurs in the solid materials through the application of a high voltage, resulting in selective crushing of the materials' boundaries. In the EHD mechanism, shockwaves derived from breakdown in solution result in physical destruction of the materials. Further investigations are needed but the contributions of the two different mechanisms were optimized in the above condition. The glass layer consisted of glass, encapsulant, the silicon substrate, bus-bar electrode and finger electrodes. The back sheet layer was composed of the bus-bar electrode, encapsulant, and back sheet. We considered that more effective results might be obtained by conducting a secondary crushing step for each layer after separation of the panel into two layers.

~~To elucidate the separation mechanism of the panel into two layers, we observed fracture surfaces after the first crushing step, under the optimal conditions, by scanning electron microscope (SEM; VE-9800, Keyence, Japan) and energy-dispersive X-ray spectroscopy (EDX; EDAX Genesis, Ametek Co. Ltd., Japan).~~ Figure 3 shows SEM and elemental mapping images of a fracture surface of the back sheet layer. The Al particles

shown in Fig. 3(a) were spherical in shape and bound together [Fig. 3(b)]. We considered that the Al particles, such as those shown in Fig. 3(a), were bound by heat or physical stress to give the morphology observed in Fig. 3(b). It has been reported that selective separation by this crushing technology results from microexplosions and stress (Kamata et al., 2016). Therefore, these results suggest that separation of the panel was caused by heat generated from microexplosions or by physical stress from shock waves in the Al electrode and Si substrate. This behavior is characteristic of high-voltage pulse crushing technologies; it is assumed that other crushing technologies will not separate panels into two layers in such a manner.

Secondary crushing step

Figure 4 shows the products obtained following the secondary crushing step of the glass layer, which also featured a large amount of encapsulant. Glass was separated from the encapsulant under all conditions and the figure shows that glass particles were effectively removed. At higher discharge voltages the encapsulant was destroyed rather than separating from the glass. To liberate materials, it is desirable for mutual separation to occur without destruction of each material. Therefore, we decided that the optimal conditions were the lowest discharge voltage of 90 kV for 250 pulses because the bus-bar electrode separated from the encapsulant under these conditions.

Figure 5 shows the fractions after crushing of the glass layer under the optimal conditions. Figures. 6 and 7 summarize the elemental compositions of each particle size fraction after crushing the glass layer under the optimal conditions (Si, Na, Ca, Mg, Al, Cu, Sn, Pb, and Ag content). Figure 8 presents the estimated compositions of each particle size

fraction after crushing under the optimal conditions. Figure 9 shows the distribution of each material after crushing under the optimal conditions. After sieving of the products obtained from the secondary crushing step of the glass layer, the glass was mainly distributed in 45–850 μm size fraction with a smaller content of Si powder: The distribution ratio of glass in the size fraction was greater than 85.0% and the purity of glass was greater than 95.2%. For glass and Si powder, the 150–300 μm size fraction had the largest weight percentage followed by that of the 300–500 μm fraction. To separate these fractions into glass and Si powder, a physical separation process other than sieving was necessary. The 500–1000 μm size fraction mainly contained glass with a small amount of impurities. The distribution ratio of Cu+Sn+Pb in the size fractions of 1.0–2.0, 2.0–4.0, and 4.0–8.0 mm was greater than 90% because these particle sizes contained the bus-bar electrode. Although the contents of Cu+Sn+Pb was as low as 16.8% in these fractions, we expected that encapsulant (content: 19.6%) could be easily separated owing to its lower density. Notably, the other impurities (content: 63.6%), e.g., glass and silicon, would not be a problem for recovery of these metals in the copper refining process. The Ag used in the finger and bus-bar electrodes was highly condensed in the sieved product fractions with sizes less than 20 μm, 2.0–4.0, and 4.0–8.0 mm, and the contents accounted for more than 3,000 mg/kg. In these fractions, Ag accompanies the above-mentioned electrode metals (Cu+Sn+Pb), and Ag can be recovered in the Cu refining process in anode slime in the Cu electrorefining process. However, the total amounts of Ag in these fractions accounted for only 33.2% of the total Ag in the panel; thus, to increase the Ag recovery ratio, other separation methods will be needed.

Figure 10 shows the products obtained from the secondary crushing step of the back sheet layer, which were mainly derived from the large back sheet. The bus-bar electrode was separated from the back sheet under all investigated conditions. At 90 kV, the bus-bar electrode was separated after 200 pulses. In terms of mutual separation of the back sheet, which consisted of resins, a lower discharge voltage was advantageous for separation of the resins over a higher voltage.

Dense medium separation

We investigated dense medium separation as a method to purify glass and concentrate Ag to increase the recovery rates. This method uses density rather than particle size to separate components.

Dense medium separation of the 300–500 μm sieved product fraction at a specific gravity of 2.4 was conducted to purify glass (2.5 g/cm^3) and remove Si powder (2.3 g/cm^3). Figure 11 shows the content ratios of the materials in each product fraction after dense medium separation of the 300–500 μm sieved product fraction. In the light product, Si powder was the main constituent at 77.9 wt%. The heavy product was almost completely glass; the impurity concentration in the heavy product was just 0.7 wt%. The Ag concentration of the light product was 1,900 mg/kg, which was much higher than that before separation. We consider that the Ag concentration in the light product was high because Ag adhered to Si particles as shown in Figure 1. The inconsistency in mass balance, before and after dense medium separation experiments, was attributed to

experimental error from the small sample of approximately 100 mg, and mass loss owing to small particles adhering to the experimental instruments.

Dense medium separation of the sieved product fraction with a size of less than 20 μm at a specific gravity of 3.0 was performed to concentrate Ag (10.5 g/cm^3) and remove glass (2.5 g/cm^3), and Si powder (2.3 g/cm^3). Figure 12 shows the content ratios of materials in each product fraction after dense medium separation of the sieved product fraction with a size of less than 20 μm. The content ratios of materials in the light product and before separation were almost the same and the Ag concentrations were both 0.3 wt%. Conversely, the Ag concentration in the heavy product was 9.7 wt%, which was more than 30 times that before crushing.

Cost evaluation for electrical-pulse crushing treatment

The process cost was evaluated from the monitored discharge energy used in the high-voltage pulse crushing under the optimal conditions. The optimal conditions were determined as the following discharge voltage and pulse number: primary crushing step, 110 kV for 20 pulses; secondary crushing step of the glass layer, 90 kV for 250 pulses; secondary crushing step of the back sheet layer, 90 kV for 200 pulses. The sum of discharge energies under the optimal conditions was 21.2 kJ. The cost was evaluated assuming an electricity cost of 13.5 Japanese yen (JPY)/kWh (about 0.123 USD/kWh) and scaled in relation to the relative sizes of the experimental samples and real panel. As a result of the evaluation, the processing cost of high-voltage pulse crushing was estimated to be 0.21 JPY/W (about 0.0019 USD/W). This estimated cost was low and suggests

promise because the targeted process cost suggested by the New Energy and Industrial Technology Development Organization (NEDO) is 5 JPY/W (about 0.045 USD/W) (Research Evaluation Committee of New Energy and Industrial Technology Development Organization, 2017).

Conclusions

In this study, we crushed a photovoltaic panel by high-voltage pulse crushing and then separated the products by sieving and dense medium separation with the aim of selective separation and recovery of various materials in the panel. The panel was separated into glass and back sheet layers by high-voltage pulse crushing of the Al electrode and Si substrate. The optimal conditions for separation of the panel into two layers (primary crushing step) were 110 kV for 20 pulses because the layers retained their form.

We conducted a secondary crushing step of the glass layer after initial crushing under the optimal conditions. The optimal conditions of the secondary crushing step for the glass layer were 90 kV for 250 pulses because the encapsulant was mostly retained, and the bus-bar electrode was separated from the encapsulant effectively. The obtained products were then separated by sieving. Glass was mainly distributed in the 45–850 μm size fraction with small content of Si powder. Base metals, such as Cu, Sn, and Pb could be recovered in the larger size fraction (1.0–8.0 mm). The Ag concentration of the sieved product fractions was over 3,000 mg/kg, in size factions of less than 20 μm, 2.0–4.0, and 4.0–8.0 mm. We also attempted dense medium separation to increase the Ag recovery and glass purity. Purification of glass by dense medium separation at a specific gravity of 2.4 could

be achieved, where the Ag was much condensed in the light product. Through Ag condensation by dense medium separation at a specific gravity of 3.0, the Ag concentration in the heavy product was over 30 times higher than that before separation. Overall, these results suggest that a combination of high-voltage pulse crushing and physical separation is a promising approach for recycling photovoltaic panels. Furthermore, processing costs in the high-voltage pulse crushing were estimated to be 0.21 JPY/W (about 0.0019 USD/W), which shows potential for commercial viability.

Acknowledgements

This research was supported by the Environment Research and Technology Development Fund (3K162004) of the Ministry of the Environment, Japan. We thank Andrew Jackson, PhD, from Edanz Group (www.edanzediting.com/ac) for editing a draft of this manuscript.

References

Akimoto, Y., Iizuka, A., Shibata, E., Basic study on high-voltage pulse crushing of polycrystalline silicon photovoltaic panel. Proc. MMIJ Annual Meeting: Vol. 4, No. 1, [1201-11-01]; Sep 26–28; Sapporo, Japan 2017.

Bergera, W., Simona, F.G., Weimanna, K., Alsemab, E.A., 2010. A novel approach for the recycling of thin film photovoltaic modules. Resour. Conserv. Recycl. 54, 711–718.

Dodbiba, G., Nagai, H., Wang, L.P., Okaya, K., Fujita, T., 2012. Leaching of indium from obsolete liquid crystal displays: Comparing grinding with electrical disintegration in context of LCA. Waste Manag. 32, 1937–1944.

Doi, T., Tsuda, I., Unagida, H., Murata, A., Sakuta, K., Kurokawa, K., 2001. Experimental study on PV module recycling with organic solvent method. Sol. Energy Mat. Sol. Cells. 67, 397–403.

Duan, C., Diao, Z., Zhao, Y., Huang, W., 2015. Liberation of valuable materials in waste printed circuit boards by high-voltage electrical pulses. Miner. Eng. 70, 170–177.

Goe, M., Gaustad, G., 2014. Strengthening the case for recycling photovoltaics: An energy payback analysis. Appl. Energy. 120, 41–48.

Granata, G., Pagnanelli, F., Moscardini, E., Havlik, T., Toro, L., 2014. Recycling of photovoltaic panels by physical operations. Sol. Energy Mat. Sol. Cells. 123, 239–248.

IEA-PVPS, 2017. Trends 2017 in Photovoltaic Applications - Survey Report of Selected IEA Countries between 1992 and 2016.

Kamata, Y., Owada, S., Namihira, T., Nakamura, T., Clarifying the mechanism of selective breakage at phase boundary in electrical disintegration by using binary artificial samples. Proc. MMIJ Annual Meeting: Vol. 3, No. 1, [1602]; Mar 28–30; Tokyo, Japan, 2016;

Kang, S., Yoo, S., Lee, J., Boo, B., Ryu, H., 2012. Experimental investigations for recycling of silicon and glass from waste photovoltaic modules. Renew. Energy. 47, 152–159.

Kim, Y., Lee, J., 2012. Dissolution of ethylene vinyl acetate in crystalline silicon PV modules using ultrasonic irradiation and organic solvent. Sol. Energy Mat. Sol. Cells. 98, 317–322.

Klugmann-Radziemska, E., Ostrowski, P., 2010. Chemical treatment of crystalline silicon solar cells as a method of recovering pure silicon from photovoltaic modules. Renew. Energy. 35, 1751–1759.

Klugmann-Radziemska, E., Ostrowski, P., Drabczyk, K., Panek, P., Szkodo, M., 2010. Experimental validation of crystalline silicon solar cells recycling by thermal and chemical methods. Sol. Energy Mat. Sol. Cells. 94, 2275–2282.

Radziemska, E., Ostrowski, P., Cenian, A., Sawczak, M., 2010. Chemical, thermal and laser processes in recycling of photovoltaic silicon solar cells and modules. Eco. Chem. Eng. S. 17, 385–391.

Research Evaluation Committee of New Energy and Industrial Technology Development Organization, 2017. Interim Evaluation Report of “Technology Development Project for Recycling of Photovoltaic Power Generation”.

Wang, E., Shi, F., Manlapig, E., 2011. Pre-weakening of mineral ores by high voltage pulses. Miner. Eng. 24, 455–462.

Wang, E., Shi, F., Manlapig, E., 2012. Mineral liberation by high voltage pulses and conventional comminution with same specific energy levels. Miner. Eng. 27–28, 28–36.

Weckend, S., Wade, A., Heath, G., 2016. End-of-Life Management: Solar Photovoltaic Panels.

Zhao, Y., Zhang, B., Duan, C., Chena, X., Sunb, S., 2015. Material port fractal of fragmentation of waste printed circuit boards (WPCBs) by high-voltage pulse. Powd. Tech. 269, 219–226.

Captions List

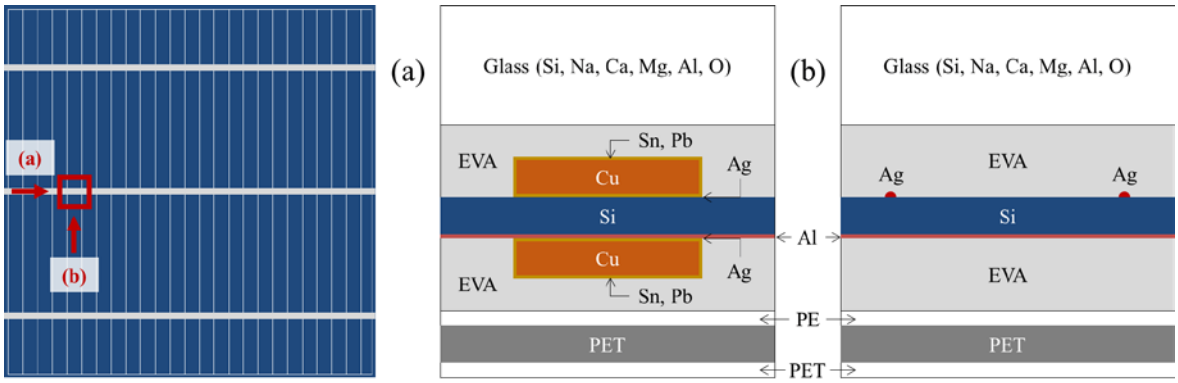

Fig. 1 Cross-sectional diagrams of the photovoltaic panel used in this study. (a) Cross section in the direction with a bus-bar electrode; and (b) Cross section in the direction with a Ag finger electrode (cited from Akimoto et al., 2017 and partly revised).

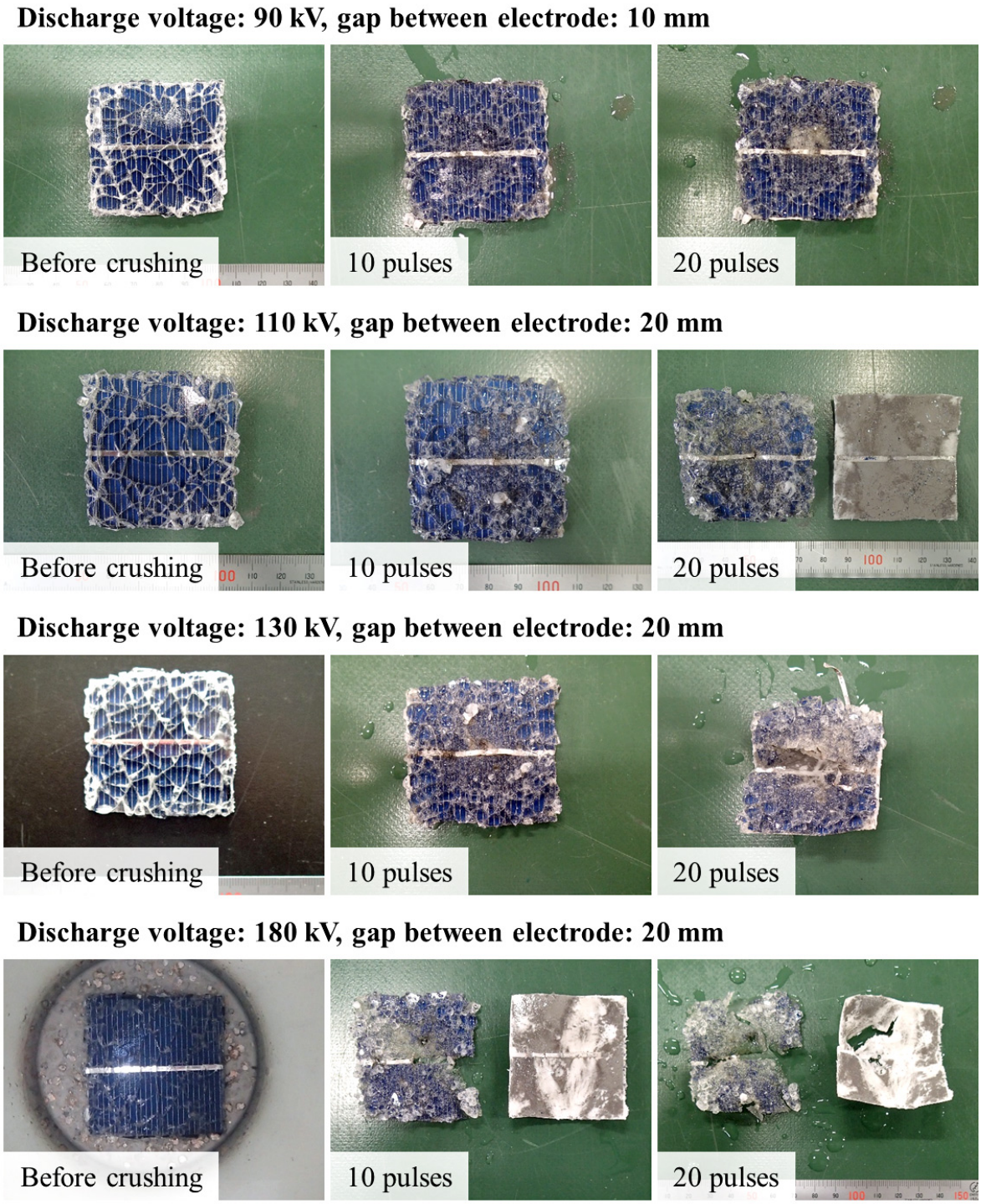

Fig. 2 Products obtained from the primary crushing step under various conditions.

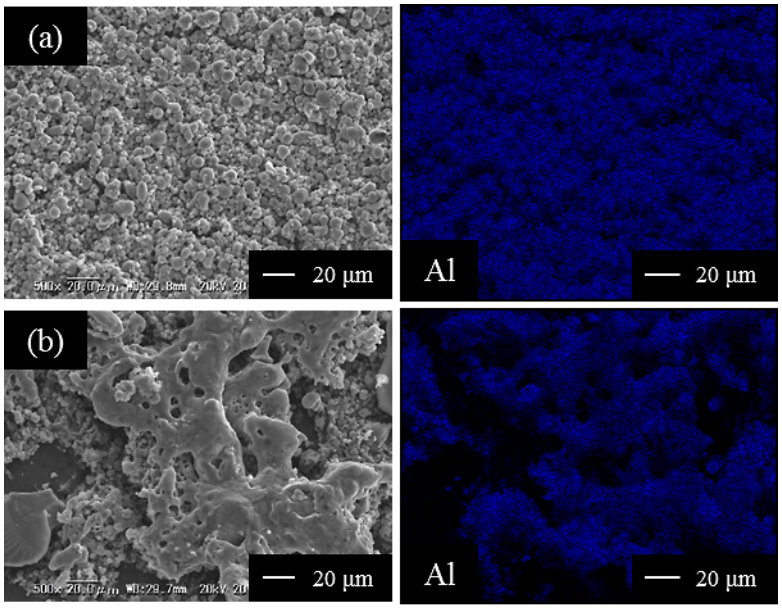

Fig. 3 SEM (left) and elemental mapping images (right) of the fracture surface of the back sheet layer.

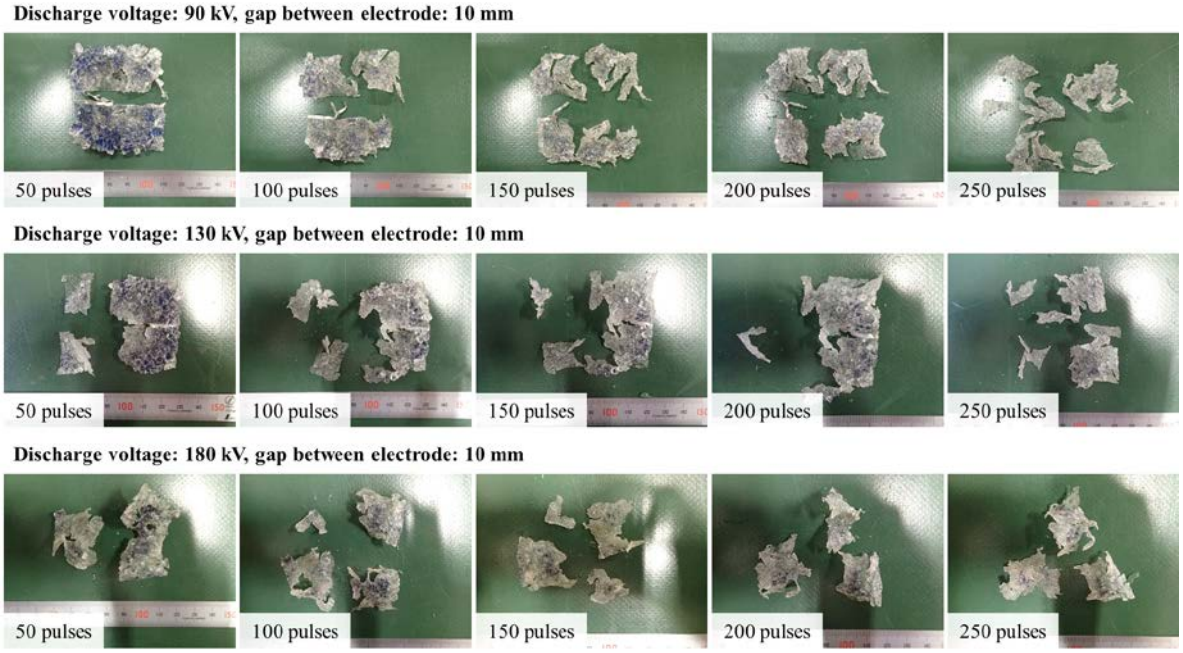

Fig. 4 Products obtained from the secondary crushing step of the glass layer. (glass particles were removed)

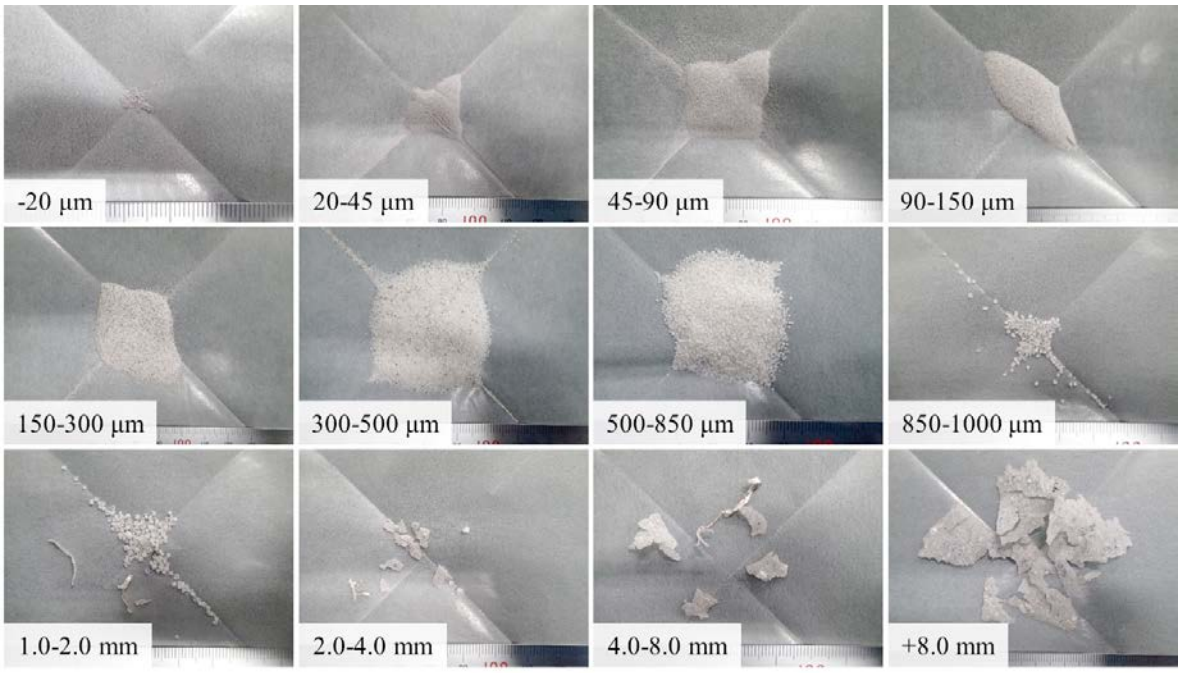

Fig. 5 Fractions after crushing of the glass layer under the optimal conditions.

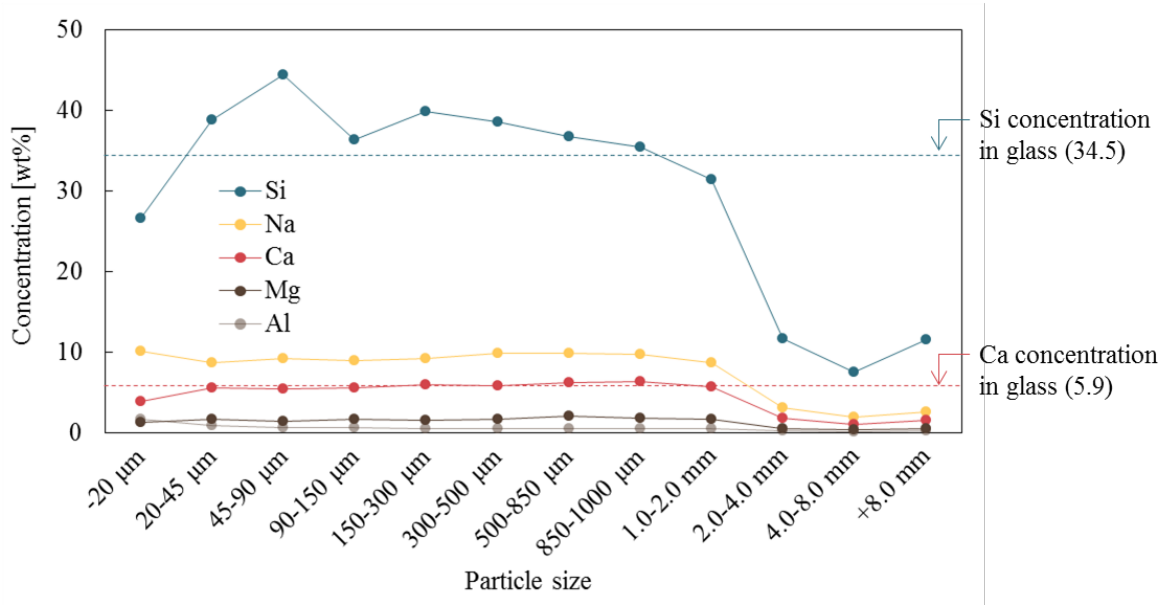

Fig. 6 Elemental compositions of each particle size fraction after crushing the glass layer under the optimal conditions (Si, Na, Ca, Mg, and Al content).

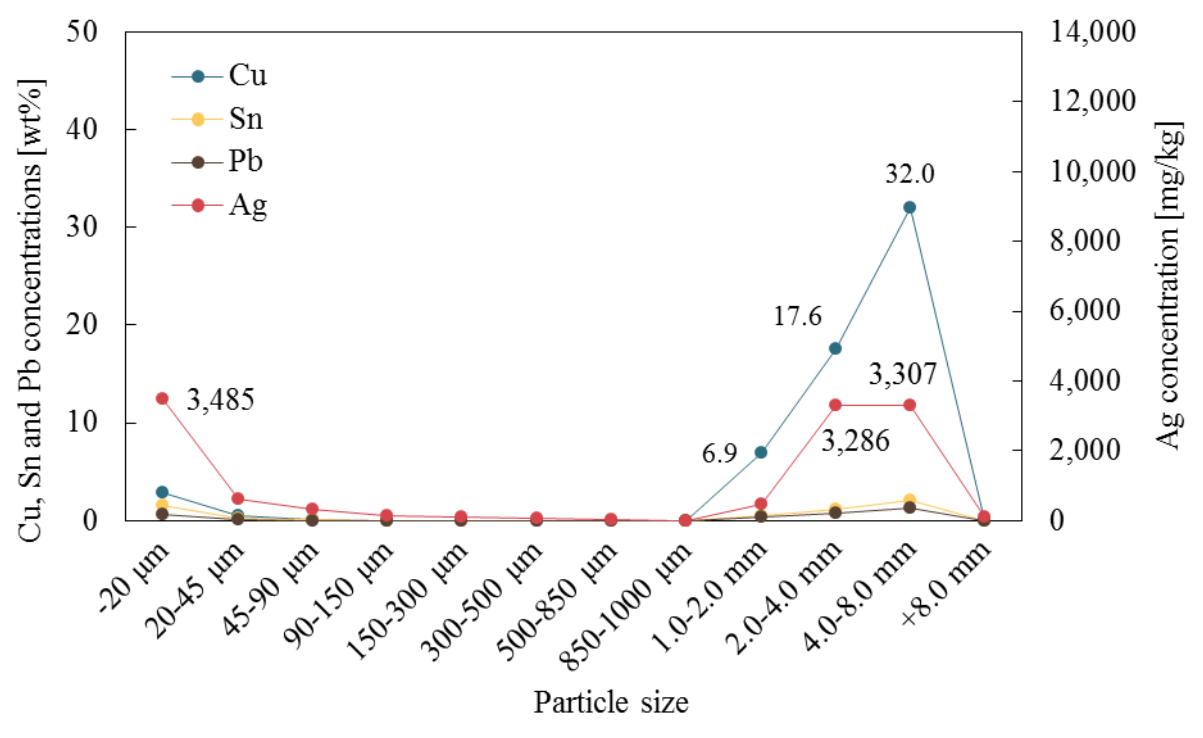

Fig. 7 Elemental compositions of each particle size fraction after crushing the glass layer under the optimal conditions (Cu, Sn, Pb, and Ag content).

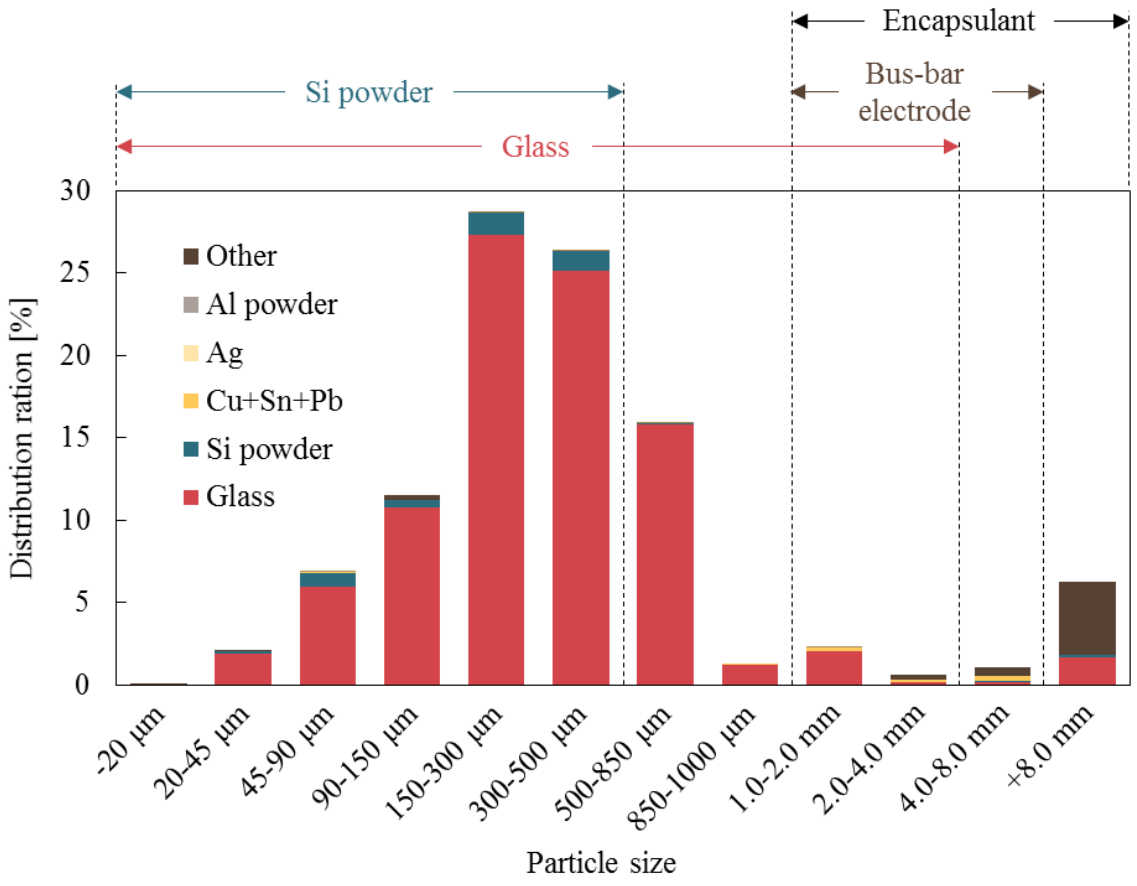

Fig. 8 Estimated compositions of materials in each particle size fraction after crushing the glass layer under the optimal conditions.

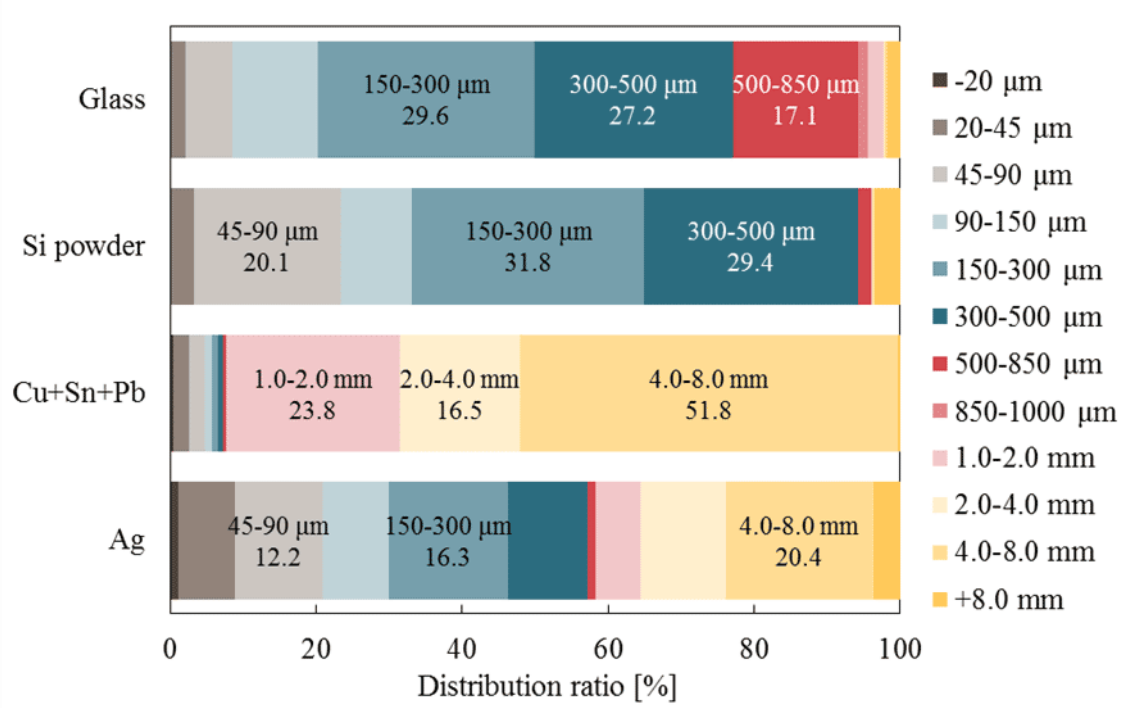

Fig. 9 Distribution of each material after crushing of the glass layer under the optimal conditions.

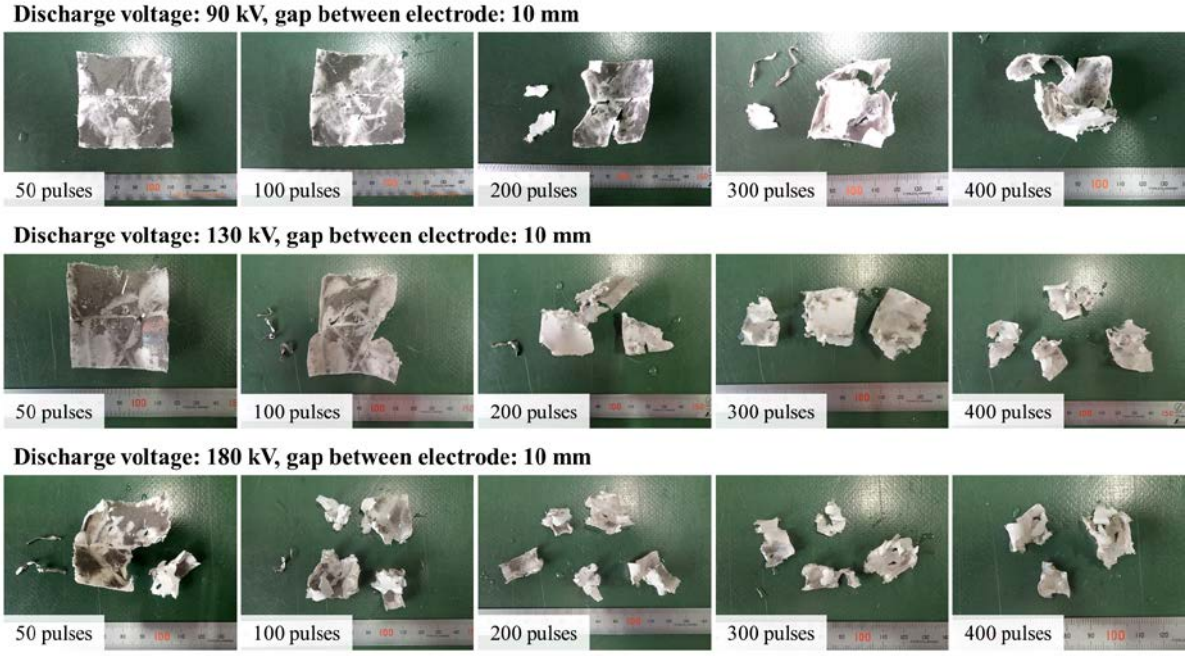

Fig. 10 Products obtained from the secondary crushing step of the back sheet layer.

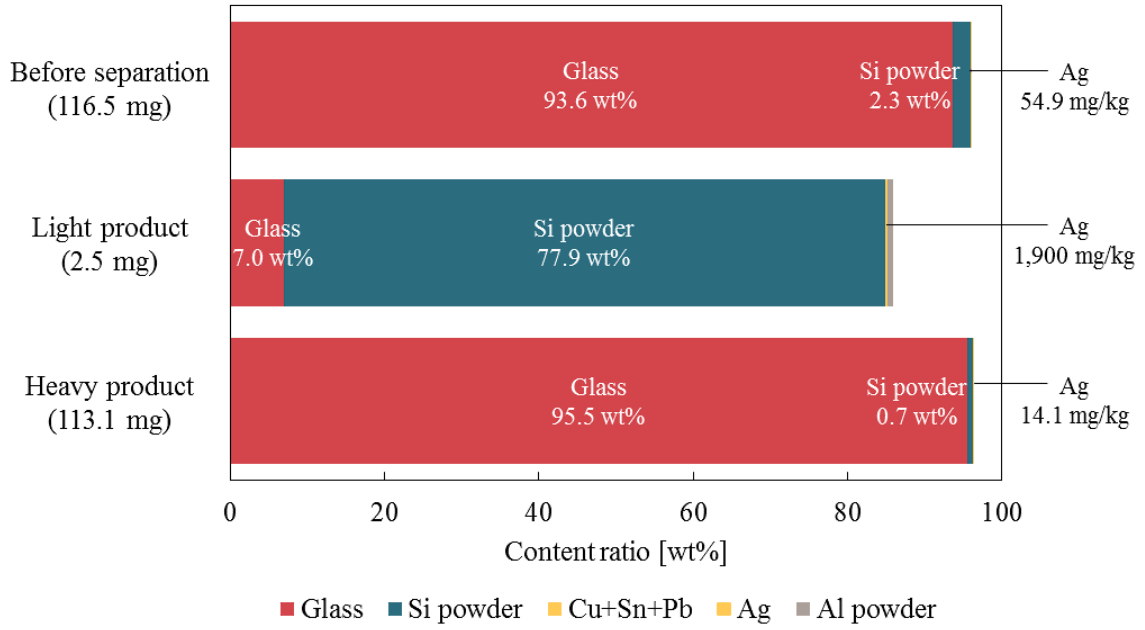

Fig. 11 Content ratios of materials in each product fraction after dense medium separation of the 300–500 μm sieved product fraction.

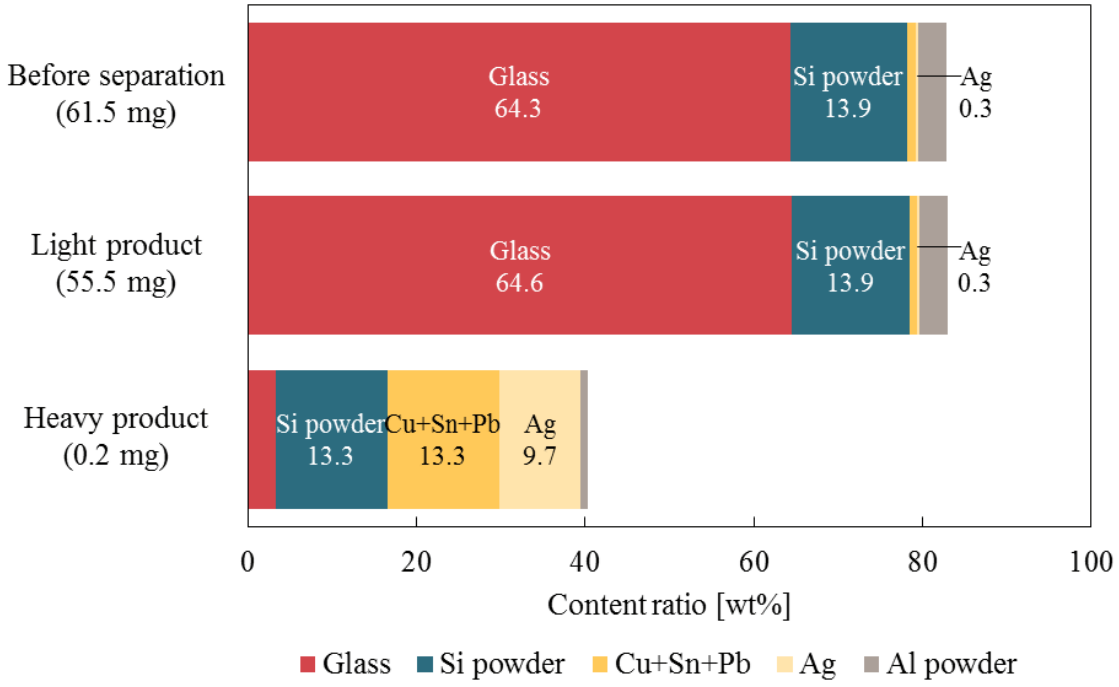

Fig. 12 Content ratios of materials in each product after dense medium separation of the sieved product fraction with a size of less than 20 μm.

Table 1 Content of each material in cut photovoltaic panel samples (wt%).

	Glass	Si substrate	Cu	Sn	Pb	Ag	Al electrode
Glass	77.7	-	-	-	-	-	-
Bus-bar electrode (Upper surface side)	0.00009	0.001	0.55	0.057	0.042	0.010	0.000008
Bus-bar electrode (Bottom side)	0.0002	0.004	0.55	0.056	0.040	0.003	0.00007
Other	0.62	4.0	0.0006	0.0009	0.0008	0.025	0.19
Total	78.4	4.0	1.1	0.11	0.083	0.038	0.19

Table 2 Experimental conditions in the primary crushing step.

Discharge voltage [kV]	Gap between electrodes [mm]	Discharge frequency [Hz]	Total pulse number [-]
90	10	5	20
110	20	5	20
130	20	5	20
180	20	5	20

Table 3 Experimental conditions in the secondary crushing step.

Discharge voltage [kV]	Gap between electrodes [mm]	Discharge frequency [Hz]	Total pulse number for the glass layer [-]	Total pulse number for the back sheet layer [-]
90	10	5	250	400
130	10	5	250	400
180	10	5	250	400